1.1 Introduction

Nanomaterials (NMs) are the foundation of nanoscience, engineering, and nanotechnology. In the last few decades, NMs are one of the attractive research areas in the various branches such as physical, biological chemical sciences and engineering[1, 2]. The "nano" term comes from the Greek word; it means dwarf and it is referring to the size 10^{-9}meter =1 nanometer (nm); it means one billion nm is equal to one meter. The average size of nanostructure materials generally has 1-100 nm [3, 4]. The birth of "nanomaterial" is in 1959 and it is given by physicist scientist Richard Feynman [5]. The nanotechnology term first time was introduced by Prof. Norio Taniguchi of Tokyo Science University Japan in 1974 [6]. The nanostructure materials display new and improved physical properties of materials when reducing the size from bulk to nano in one or more dimension. These unique features of materials can be utilized for different thin film device applications. Beside different electronics application, nanostructure materials play a significant role in various filed such as medical sciences, agriculture and environmental science as well [4, 7-9].

1.2 Classification of nanostructure materials

The nanostructure materials have different types of shape such as lamellar thin film, atomic cluster, filamentary nanostructures etc. Accordingly, nanostructure materials are classified in different name based on their structure. Commonly these classification of nanostructure materials are named as zero dimension (0D), one dimension (1D), two-

dimension (2D), and three-dimension (3D) nanostructured materials which are shown in figure (1.1) and explain below [1, 4, 10-12].

1.2.1 Zero dimensions (0D) nanostructure materials

These nanostructure materials are usually called as nanparticles due to their particle like spherical shape within 100 nm size. In case some semiconductor nanoparticles becomes too small so that the quantum confinement phenomena can occur in all three directions. In that particular case, specifically those semiconductor nanoparticles are called as quantum dots. The number of electronic states of any energy band of a semiconductor per unit energy is called density of state (DOS), and this DOS for the quantum dots looks like a Dirac delta function (DOS α $\delta(E)$), which shown in figure 1.1.

1.2.2 One dimension (1D) nanostructure materials

In this nanostructure, two dimensions of nanomaterial are within 100 nm scale and other the dimension is higher than those. These 1D nanostructures materials are classified as nanowires, nanotubes and quantum wires, based on their structure. In some 1D semiconductor nanosctructure materials those two dimensions can be too low so that quantum confinement effect can be observed. In those 1D semiconductor nanostructures the DOS is proportional to the $\mathbf{E^{-1/2}}$ which shown in figure 1.1 is called the quantum wire.

1.2.3 Two dimension (1D) nanostructure materials

This class of nanostructure material has one dimension within 100 nm range where as two other dimensions are much higher than that. Some of those 2D nanostructure materials may show the electron confinement in the one dimension is commonly called

quantum sheet. The DOS of that quantum sheet is a step function as shown in shown in the figure1.1.

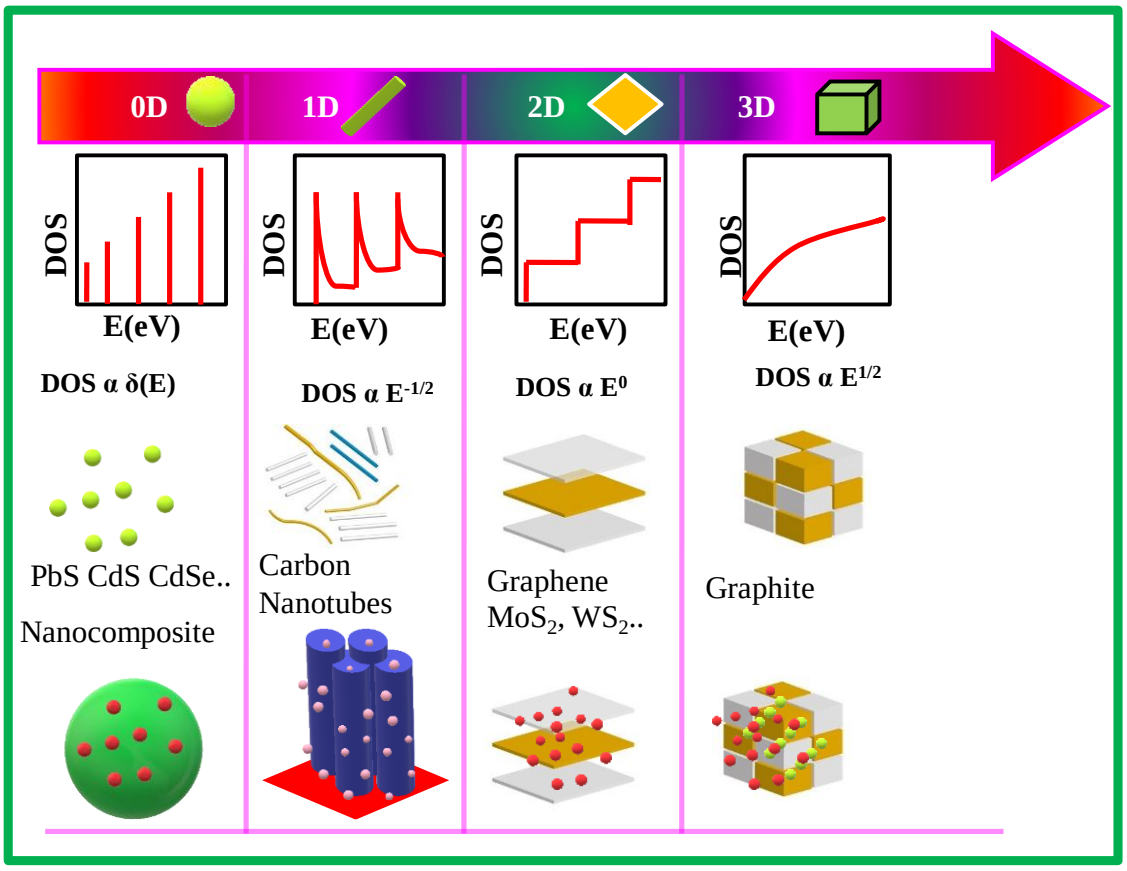

Figure 1.1: *The classification of nanostructured materials based on quantum confinement, shape, and size.*

1.2.4 Three dimensions (3D) nanostructure materials

In 3D nanostructure materials, there is no confinement in three-dimension. Although all three dimensions of this nanostructure are with 100 nm scale. For examples are nanocubics, fullerenes in three dimensions. The DOS of these 3D nanostructures is directly proportional to the $\mathbf{E^{1/2}}$.

Beside that dimension issue, nanostructure materials can be classified in two categories based on the nature of electrical conductor. One of them is metallic and the other

one is nonmetallic nanostructure [13-16]. Examples of these two categories are shown in figure 1.2.

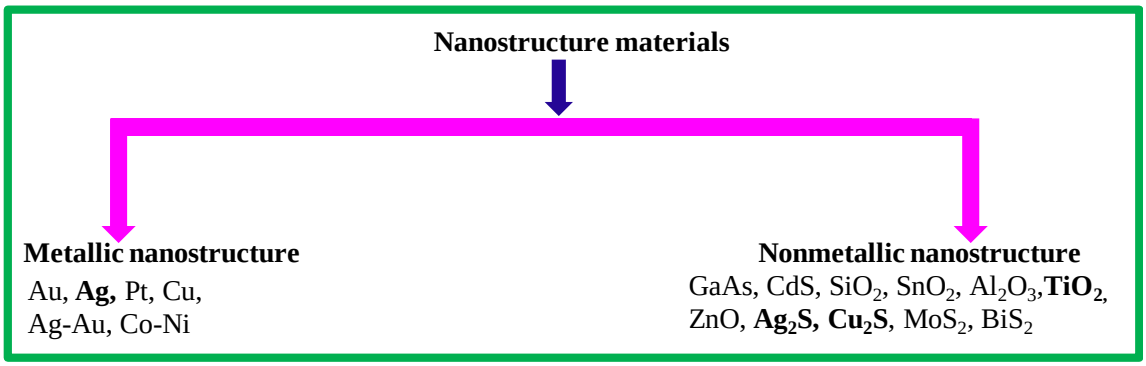

Figure 1.2: *The classification of nanostructured materials based on the materials.*

Example of metallic nanostructure materials: Silver (Ag), gold (Au), copper (Cu), platinum (Pt), and palladium (Pd), etc. and alloys with combination of two metals like Ag-Au, Pt-Pd end so on [17-20].

Example of nonmetallic nanostructured materials: **Titanium oxide (TiO_2),** zinc oxide (ZnO), tin oxide (SnO_2),silicon oxide (SiO_2), etc., Metal sulfide nanostructured materials are included **silver sulfide (Ag_2S), copper sulfide (Cu_2S)**, tungsten sulfide (WS_2), molybdenum oxide (MoS_2), lead sulfide (PbS), cadmium sulfide (CdS), and cadmium selenide (CdSe), etc [3, 21-24].

1.3 Application of nanostructured materials

The nanostructure materials have the different application in the various areas including energy harvesting (like solar cell, electrocatalyst, photocatalytic, photoelectrocatalytic, solar-thermal collector etc.), electronic devices (mobile phone, transistor, display technology, sensor etc), environmental and agriculture and biomedical application. A

summary of different application of nanostructure materials is shown in the figure (1.3) [8, 25-32].

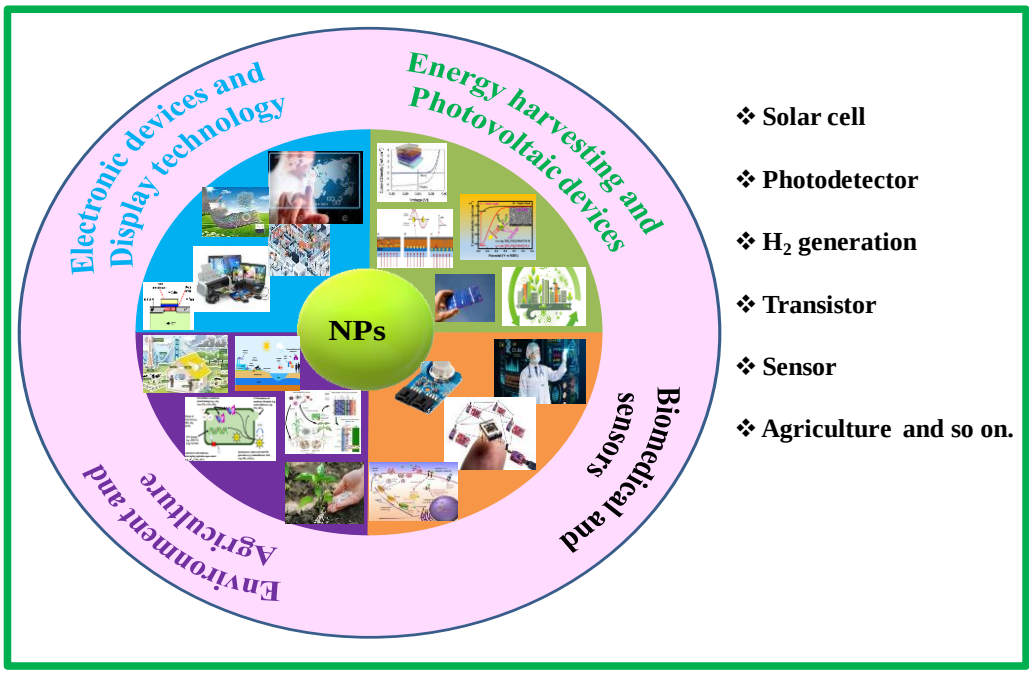

***Figure 1.3**: The application of nanostructured materials*

1.3.1 Energy harvesting

Solar cell: In a nanocrystal based solar cell device, nanocrystal is used as active light absorbing material. These nanocrystals are typically based on silicon, PbS, CdTe or CIGS and the substrates are generally ITO coated glass or silicon. Quantum dot solar cells are also nanocrystal based solar cell, but that take advantage of quantum confinement effects to extract further performance. Quantum dot-sensitized solar cells are another class of nanocrystal based solar cell, where colloidal quantum dots are used as sensitizer of the device. Nanocrystal can be deposited by different physical vapour deposition as well as various solution processed technique.

Electrocatalysis: Electrocatalyst enhance the reaction rates by lowering the energy barrier for electrochemical reactions that is taking place at the surface of electrodes. Beside,

electrocatalyst also promote the charge transfer process that takes place on the surfaces. To enhance this electrochemical reaction, the development of novel materials with high activity and stability for electrocatalysis is considered to be the most important factors. Generally, these catalytic reactions occur on the active sites of catalysts, in which the low coordinated steps, edges, terraces, kinks and corner atoms are often the favorable catalytic reaction sites. Nanostructured materials have high surface-to-volume ratio with dominant facets. Because of these reasons nanostructure materials have emerged as an ideal platform for providing molecular/nanoscale insights into the relationships between active site and catalysis.

Photocatalytic: Nanocrystal based photocatalytic systems are based on different colloidal semiconductor nanocrystals due to their potential benefits that include a visible-range light extinction and a low spatial overlap of photo induced charges. These nanocrystals can be pure metal oxide based or metal/metal oxide heterojunction nanocrystal. When a metal oxide is coupled to metal catalysts, nanocrystal sensitizers have demonstrated a compelling performance in homogenous photoreduction reactions, including the degradation of organic dyes and hydrogen generation. Example of homogeneous nanocrystal that are commonly used for photocatalytic applications are TiO_2, perovskite oxide etc. On the other hand Ag/TiO_2, Au/TiO_2 is commonly used as metal/metal oxide junction nanocrystal for this application. However, instead of a significantly efforts, so far the progress of nanocrystal based photocatalysis is still very limited due to different critical issues.

Photoelectrocatalytic: In photoelectrochemical (PEC) cell that is used for water splitting in presence of sunlight, external bias and specialized semiconductors called photoelectrochemical materials. This cell is capable to convert electromagnetic energy

(light) to directly dissociate water molecules into hydrogen and oxygen. This is a long-term technology pathway, with the potential for low or no greenhouse gas emissions. The PEC water splitting process uses different types of metal-oxide semiconductor materials to convert solar energy directly to chemical energy in the form of hydrogen. These metal-oxide semiconductor materials are mostly wide band gap that chemically and environmentally stable. However, due to their wide band gap nature, these oxide semiconductors can absorb only high energy photons like deep blue of UV light. To improve the efficiency of this PEC, metal/metal oxide heterojunction are commonly formed which is capable to enhance the absorption spectra of the PEC cell via LSPR phenomena. Again, this absorption spectrum can be enhanced by forming a heterojunction with a lower band gap semiconductor.

Solar-thermal collector: Major issue of solar-thermal energy harvesting is to improve the efficiency of solar collectors by enhancing the thermal conversion efficiency of transporting fluid. Conventional heat transporting fluids of a solar-thermal collector are water or oil based that have low heat absorption and heat transfer capacity. In contrast nanofluids are the fluids that contain homogeneous solution of nanoparicles of size 1 to 100 nm in base fluid. These nanofluids exhibits enhanced or modified thermo- physical properties due to their high surface to volume ratio. These thermo- physical properties are thermal conductivity, convective heat transfer coefficient, viscosity and thermal diffusivity compared to base fluids etc. In addition, nanoparticle base fluid can significantly enhances thermo physical mass diffusivity and radioactive heat transfer properties of fluid. Even with very low volume percentage of nanoparicles in base fluid remains, the impact in terms of thermal efficiency observed is very significant. Due to these inherent characteristics,

nanofluids are getting increasing attention among scientific, academic and engineers to develop improved systems and devices which are based on nanofluids as a heat transporting and absorbing medium.

1.4 The properties of nanostructure materials

Due to the reduction of thesize (in dimensions) of a nanostructure material, both the physical and chemical properties of materials changes significantly from their corresponding bulk materials. These changes occur due to the (a) larger surface area (that causes the large surface energy) (b) higher surface to volume ratio(c) quantum confinement effect, (d) reduction of imperfections and (e) surface plasmon resonance (SPR) effect (for metallic nanostructure). The NMs have various forms, such as metal, semiconductors (metal oxide, metal sulfides, etc.), insulators, metal/semiconductors, and semiconductor/semiconductor nanocomposite. The physical and chemical properties of these nanostructured materials are closely related to their shape, size and their chemical composition. By changing their size, it is possible to tune their different properties including optical, mechanical, electronic, magnetic, photo-catalytic, plasmonic (for metal NPs) etc. which are listed in figure (1.4) [4, 9, 14, 33-37].

1.4.1 Optical properties

The optical properties of nanostructured materials are very different compared to their bulk size. These optical properties depends on their size, shape, and medium of the surrounding. For example, photoluminescence properties of colloidal quantum dot (QDs) can varied in a very wide range based on the size of QDs. Similarly, reflectivity and optical absorption of QDs are also strongly depends on their size [15, 38-40].

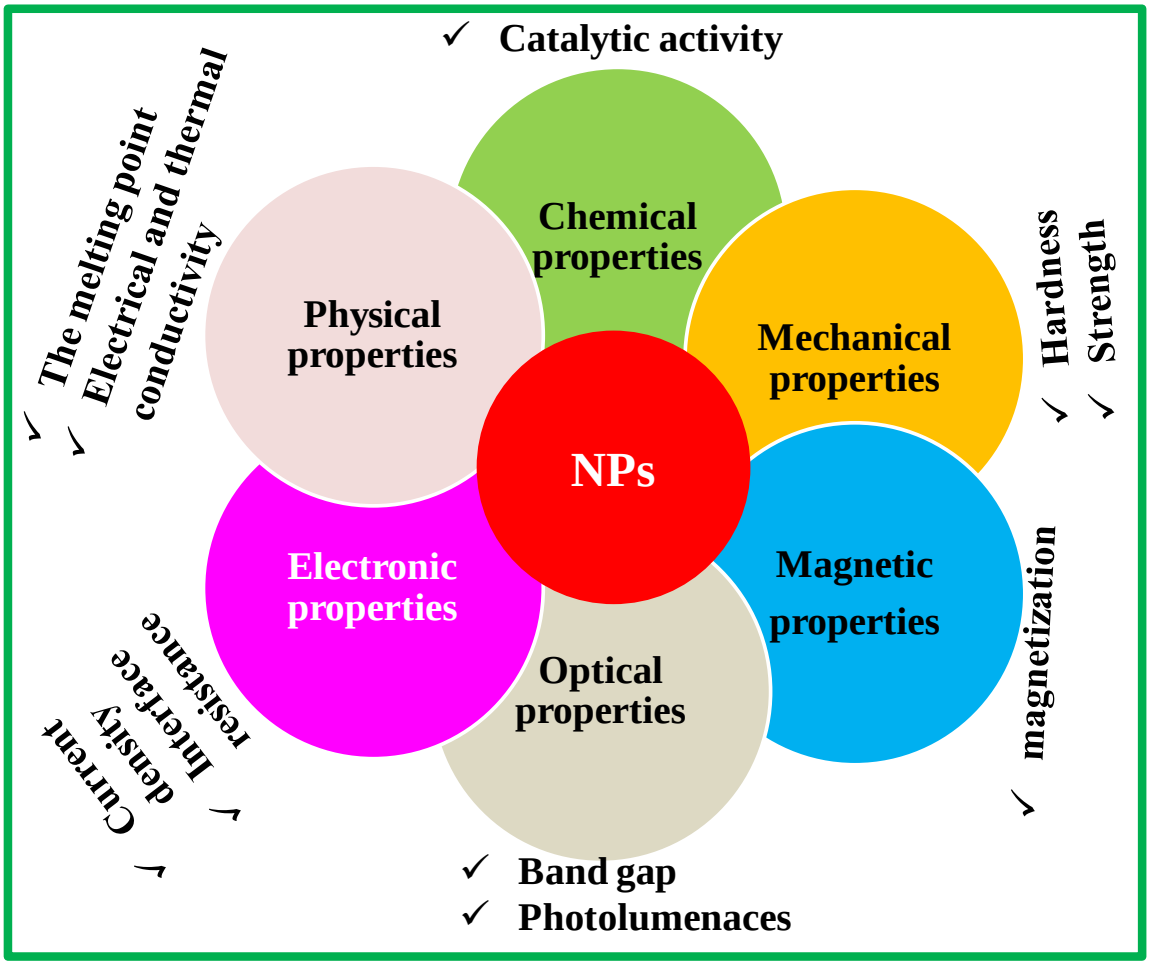

Figure 1.4: *The properties of nanostructure materials.*

Scattering, Absorption, and Extinction

When the light interacts with the nanoparticle, it can be absorbed or scattered (The sum of absorption and scattering is called attenuation or extinction). This absorbed or scattered of nanostructure materials varies greatly depending on the diameter of the particle. Absorption is a dominating phenomena for NP with lower size (<10 nm) where asscattering is the key controlling factor of extinction with larger size (100 nm). Therefore, by designing a smaller or larger diameter of the particle, it is possible to get the optimum amount of the absorption or scattering for a given material [41-43].

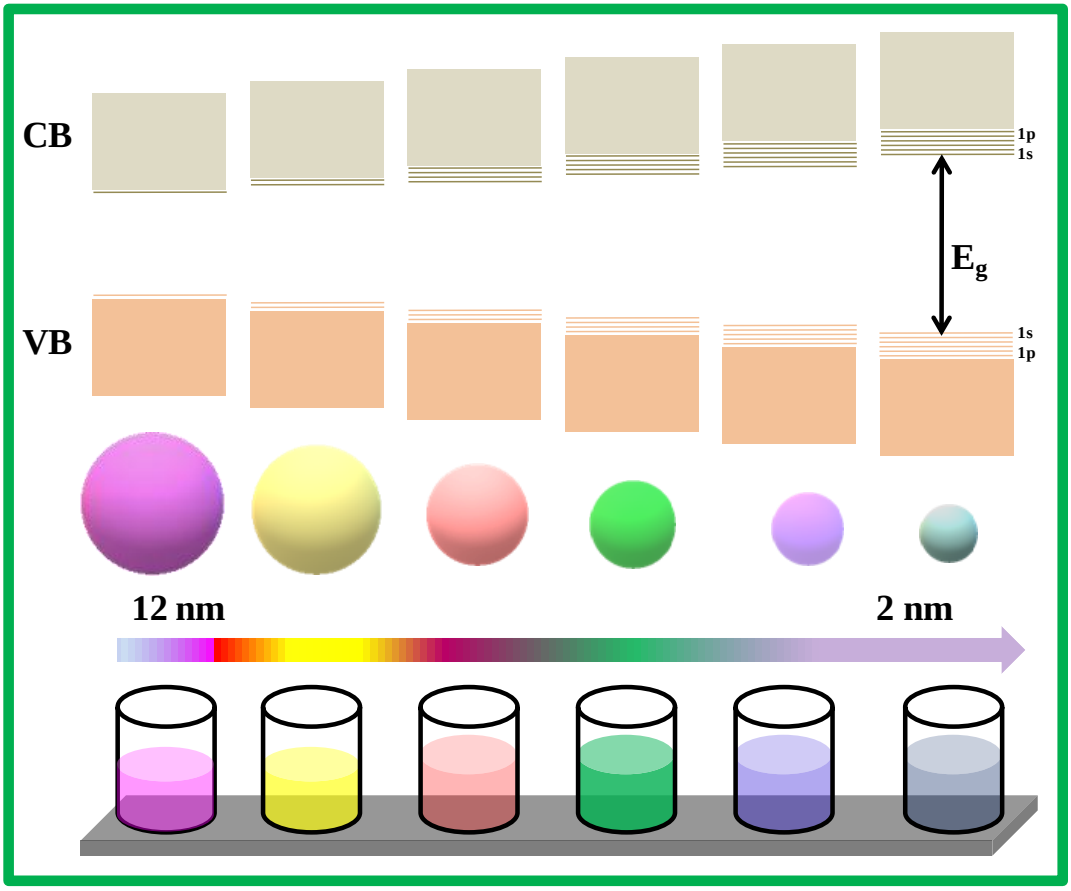

Figure 1.5: *The properties of nanostructure semiconductor materials under UV excitation.*

Tunability of the optical band gap of nanostructure semiconductor materials

The band gap of the semiconductor is an important parameter of the nanostructure materials and it can be tuned by changing the size of semiconducting NP. The band gap of the NPs depends on their size which is described in equation (1.1). Due to the variation of their band gap, the luminance properties of these materials depends on their size which is shown in figure (1.4) [37, 44].

$$E = E_{bandgap} + \frac{h^2\pi^2}{8\mu d^2} \qquad (1.1)$$

Where μ reduced mass and d is the size of the particle.

1.4.2 Plasmonic property of metallic nanostructure materials

Localized surface plasmon resonance (LSPR) is an optical property of a metal nanoparticle which is generated by a light wave trapping within the metal nanoparticles (NPs) of size smaller than the wavelength of light. As the the electric field of incident light interact collectively with the surface electrons of a metal NPs, a coherent localized plasmon oscillations with a particular resonant frequency occurs. This resonance frequency strongly depends on the composition, size, geometry, dielectric environment and separation distance of metal NPs. Because of this electron-light interaction, metal NP can absorb light efficiently at that resonance frequency which is commonly identified by UV-VIS absorption of metal NPs. Stable metal nanoparticle like Ag, Au and Cu show such kind of LSPR related absorption in visible region of light [25, 45, 46]. For example, the ruby color of spherical gold NPs in the solution is due to the strong absorption and scattering in the green region of the spectrum, while the color of Ag NPs in the solution is yellowish which is due to the surface plasmon resonance in the blue region of the spectrum [26, 47-49].

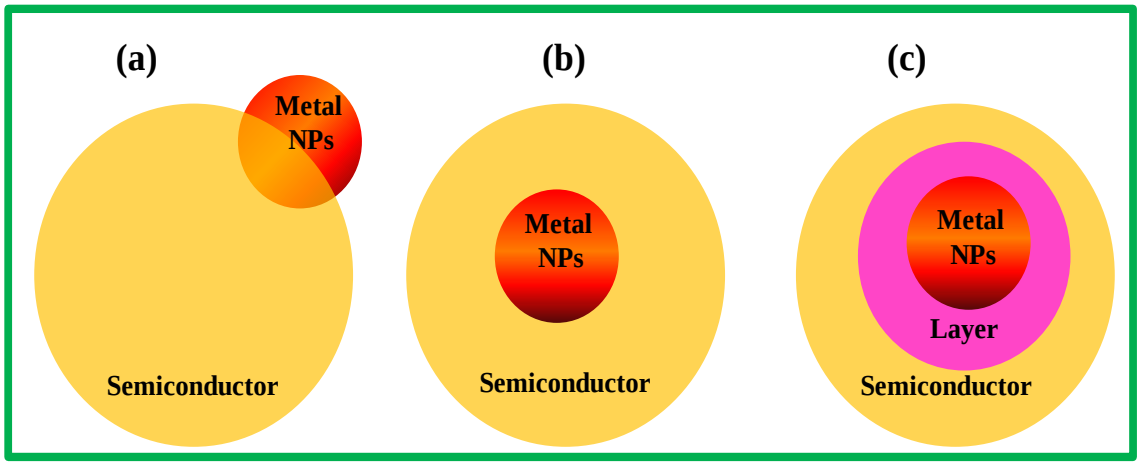

Figure 1.6: *The classification plasmonic nanostructure with semiconductor (a) the metal NPs embedded in the semiconductor (ii) the metal NPs are buried in the semiconductor, and (iii) isolated from the semiconductor.*

1.4.2.1 The classification of different plasmonic nanostructure for energy harvesting application

Metal-metal oxide nanocoposite metal-metal oxide hybride nanoparticles are used commonly used for different energy application to utilize the hot electron of metal NPs generated from LSPR. The primary aim of these different nanocomposite or hybride nanostructure is to maximize the charge collection to the metal oxide from metal NPs. Therefore the metal/semiconductor interface plays a crucial role for those applications and accordingly these nanocomposite of hybride nanostructure are classified in three different ways which is shown in figure (1.5).This classification are (i) metal NPs embedded in the semiconductor, (ii) buried in semiconductor, and (iii) isolated from the semiconductor [26, 45, 46, 50, 51].

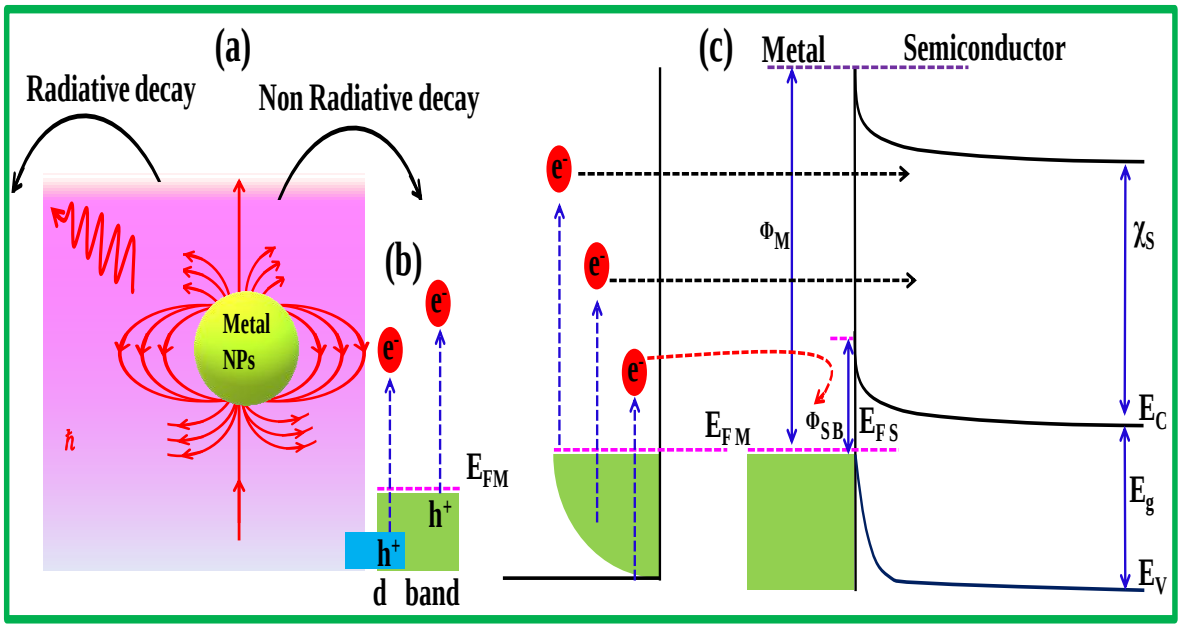

Figure 1.7: *Surface-plasmon decay, generation and injection of hot-electron in the metallic nanostructure, (a), Localized surface plasmons can decay radiatively via re-emitted photons and non-radiatively via excitation of hot electrons, (b) In plasmonic nanostructures, non-radiative decay can occur through or through interband excitations resulting from transitions between other bands (for example, d bands) and the conduction band or intraband excitations within the conduction band, (c)Plasmonic energy conversion at the metal (Ag)-semiconductor (n-TiO_2) interface.*

1.4.2.1 Plasmonic energy conversation

As mention earlier, light is absorbed by metal NPs due to the LSPR phenomena. During this process, electromagnetic energy of light is deposited to the free electron of metal NPs to form high energetic 'Hot' electron. After forming this hot electron, excess energy of electron can be release by radiative recombination and can be transfer through non-radiative decay process. In this non-radiative decay process, hot electron may transfer to the conduction band of metal oxide if its capable to overcome that barrier of metal/metal oxide junction. Plasmonic energy of metal NPs can be transferred to a semiconductor through three major mechanisms (i) hot electron injection, also named direct electron transfer (DET), (ii) the enhancement of local electromagnetic field (LEF), (iii) plasmon-induced resonance energy transfer (PIRET),(iv) the dipole-dipole coupling (v) far-field trapping/scattering and the (vi) plasmon heating effect. The direct hot-electron transfer is referred to as the injection of electrons from the metal to the conduction band of the semiconductors. The PIRET occurs when plasma oscillation is transferred at the resonance energy from the metal to semiconductor (Ag/TiO_2) via a dipole-dipole interaction. The charge generation allows due to this effect below or near the bandgap of the semiconductor and thanks to the overlapping of the bandgap and plasmonic resonance. The photothermic is the process of the plasmonic heating resulting from the decay of localized surface Plasmon resonance via electron-phonon interaction, and the gained energy of the charge carrier transfer into heat. These hot electrons have energy more than the metal/metal oxide Schottky barrier (Φ_{SB}) are injected into the conduction band of the semiconductor and shown in the figure 1.6. Different energy harvesting technology including photoelectrochemical H_2 generation, solar cell utilize these LSPR electron for improving

the efficiency of H_2 generation or power conversion efficiency of solar cell. However, there are some limitations and difficulties vested to the nature of this energy transfer process [26, 45, 46, 50, 52].

1.4.3 Basic Principle of Water Splitting via Photoelectrochemical Process

In photoelectrochemical process, light is illuminated either on a photoanode or on a photocathode which is also called the working electrode of this process. In case of n-type metal oxide semiconductor light absorbing material, anode is considered as working electrode. From the beginning of the discovery of photoelectrochemical water splitting, TiO_2 has been commonly used as semiconductor for photoanode application due to its high stability and low photo quenching effect. When high energy photon is illuminated on a photoanode, the semiconductor of the photoanode absorbs light which is greater than or equal to the band gap of the semiconductor. Due to this absorption, photo generated electron-hole (e^--h^+) pairs or excitons are formed (Fighure-1.7a). In the second step of this process, these excitons are separated to free electrons and holes. In the third step, photo generated electron is transfer to the anode which is then migrated to the counter electrode (cathode) and goes through the reduction process to form H_2 gas. On the other hand, photo generated hole carriers oxidize the water molecule to form O_2 gas in the photoanode. The complete circuit for the process shown in figure 1.7 (b), in this circuit, excited electron are transfer to the counter electron and produced the H_2 [53-56].

The band structure and redox potential are the important parameters of the H_2 or O_2 generation via water splitting. The edge of the conduction band of the semiconductors is less than 0 potential vs. NHE, which are more favorable for H_2 generation, and the edge of the valance band is more than 1.23 eV vs. NHE more suitable for O_2 evolution via water

splitting. Figure 1.7 (c) shows some important semiconductors used as photoanode for H_2, O_2, and both H_2 and O_2 evolution via water splitting. For example, gallium phosphorus (GaP) has the edge of the conduction band is negative i.e. less than zero potential, but the edge of the valance band is less than 1.23 eV, which is more suitable for H_2 generation not for O_2 evolution via water splitting. Similarly, tungsten oxide (WO_3), have the edge of the valance band, is more positive than 1.23 eV vs. NHE and the edge of the conduction band is positive, therefore, more favorable for O_2 not for the H_2 evolution via water splitting. Accordingly, the ideal positioning of the edge of the CB band potential is crucial to design for the H_2 evolution photocatalyst shown in figure 1.8(a). The TiO_2 is the best example for the HER and OER due to the edge band position of the CB and VB band [56-59], which shown in figure 1.8(b).

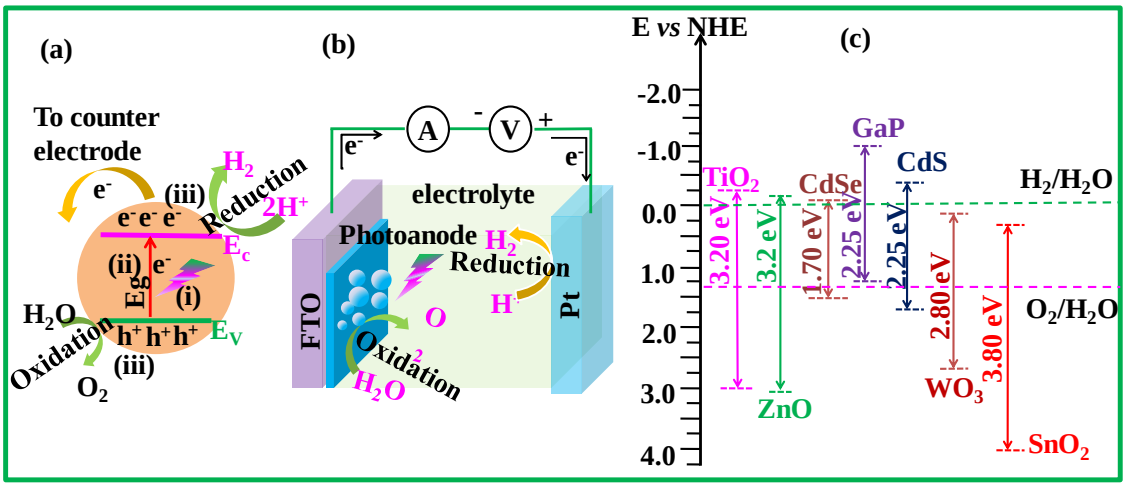

Figure 1.8: (a) *Basic principle of water splitting for H_2 generation (b) The complete circuit of the H_2 generation mechanism (c) the band structure of some semiconductor with redox potential.*

The water splitting via electrolysis into H_2 at the cathode and O_2 at the anode and these are denoted by hydrogen evolution reaction (HER), and oxygen evolution reaction (OER), respectively. These reactions are taken place in either alkaline or acidic medium as these

medium enhanced the reaction rate. The overall reactions can be processed in both media. However, the redox potential (E) of this reaction depands on the pH of the electrolyte. The equation for H_2 evaluation and O_2 evaluation at different pH are given in equation (1.3) and (1.4) respectively [56, 57, 60].

$$2H_2O + h\upsilon \longrightarrow 2H_2 + O_2 \qquad (1.2)$$

For H_2 evolution

$$\left.\begin{array}{lll} 2H^+ + 2e^- \longrightarrow H_2 & (E = 0\ V \text{ with } pH = 0) \\ 2H^+ + 2e^- \longrightarrow H_2 & (E = -0.41\ V \text{ with } pH = 7) \\ 2H^+ + 2e^- \longrightarrow H_2 & (E = -83\ V \text{ with } pH = 14) \end{array}\right\} \qquad (1.3)$$

For O_2 evolution:

$$\left.\begin{array}{lll} O_2 + 4H^+ + 4e^- \longrightarrow 2H_2O & (E = 1.23\ V \text{ with } pH = 0) \\ O_2 + 4H^+ + 4e^- \longrightarrow 2H_2O & (E = 0.81\ V \text{ with } pH = 7) \\ O_2 + 4H^+ + 4e^- \longrightarrow 2H_2O & (E = 0.41\ V \text{ with } pH = 14) \end{array}\right\} \qquad (1.4)$$

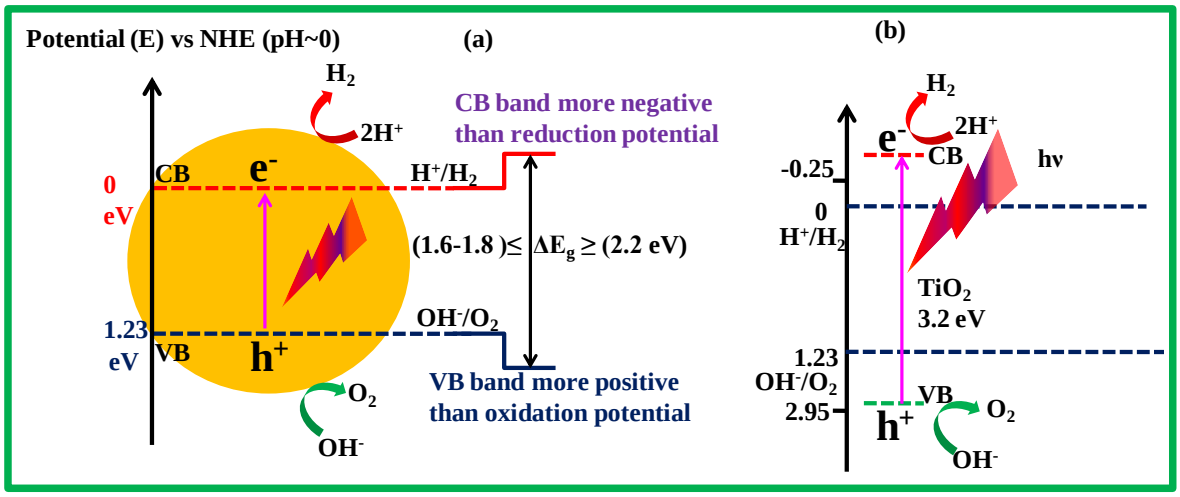

Figure 1.9: *(a) The ideal band edge positioning of H_2 and O_2 evolution photo-catalysts (b) The band edge positions of pure metal oxide (TiO_2) with respect to water redox potential towards H_2 production.*

In the photo-catalytic semiconductors, the ideal edge of the valance band (VB) potential should be more than positive of the oxidation potential (1.23 eV) and edge of the conduction band (CB) potential should be more negative of the reduction potential (0.0 eV). It is clear that the overall band gap of a semiconductor need to be more than 1.23 eV. The ideal position of the edges of the bands for the overall splitting of water molecules and the ideal band position of the photocatalyst shown in the figure 1.8(a).

1.5 Materials for photocatalytic and photoelectrocatalytic application

Wide band gap TiO_2 was first time used as photoelectrocatalysis by Fujishima and Honda in 1972 under the ultraviolet (UV) light[61]. However, due to the wide bandgap (E_g ~3.2 eV) nature of TiO_2, it was capable to absorb only UV light which is only 4-5% of total solar spectrum. Therefore, most of the light which contains the visible and infrared spectrum is not utilized for photoelectrocatalytic H_2 production via water splitting. A number of papers and review articles were published on TiO_2 based photoanode material to improve their efficiency. Different efforts have been given to modify TiO_2 by doping (cation/anion), making heterojunction with other narrow bandgap semiconductors (Ag_2S, Cu_2S, etc.) and by formatting metal/semiconductor junction which are listed in the table (1.1).

1.6 Photodetector

The detector is a device that detects the presence of a particular type of signal and converted it to some other form of signal which is realized much more easier way. When a detector detect the optical signal (light) by directly converting it to an electrical signal (current/voltage) is called a photodetector.The photodetector device can be in a various

geometry like photoconductor, photodiode, and phototransistor as shown in figure 1.10.The performance of the photodetector can be evaluated by some important parameters such as detectivity, responsivity, external quantum efficiency and response time [62-65]. A good photodetector should have high detectivity and responsivity with faster response. Whereas, quantum efficiency spectra give the sensitivity of the device at different range of wavelength.

Table 1.1: The summary of TiO_2 based photoanode with different heterojunctions

Device structure	Methods of preparation	Electrolyte and illumination condition	Current density under 100 mW/cm^2	Stability hours	H_2 production per hour	ref
Ag/TiO_2 NRA	Photo-deposition	1M KOH solution	2.5 µAcm^{-2}	-	0.55 µmolcm^{-2}	*J. Am. Chem. Soc.*, 2011, **133**, 5202-5205 [66]
Ag/TiO_2/KCN	Photo-deposition	MeOH/H_2O 1 : 10	16 mAcm^{-2}	-	250 µmolcm^{-2}	ACS Catal. 2016, 6, 821−828 [67]
Ag/n-TiO_2 Nanorod	Flame reduction method	0.5M Na_2SO_4	1.52 mA/cm^2	10	-	*Ind. Eng. Chem. Res.*, 2019, **58**, 4818-4827 [68]
Janus Au-TiO_2	Sol-gel	isopropyl alcohol/aqueous solution, (1:2)	-	-	55 ml	Adv. Mater. 2012, 24, 2310–2314[69]
Au/TiO2	Sol gel dip coating approach	glycerin ($C_3H_8O_3$)	-	-	74.56 µmolcm^{-2}	J Am Ceram Soc. 2019;102:5873–5880.[70]
Ag_2S/TiO_2		0.4 M Na_2SO_4				ACS Appl. Energy Mater. 2019, 2, 2751−2759[71]
Ag_2S/TiO_2	Sol-gel	0.5M Na_2SO_4	1.4 mA/cm^2	-	51.8 µmol cm^{-2}	Applied Catalysis B: Environmental 225 (2018) 415–423417[72]
Ag_2S/TiO_2	Photodeposition	0.05 M Na_2S +0.05M Na_2SO_3	0.35 mA/cm^2	-	0.8 mL	Langmuir 2011, 27, 7294–7300 [73]
Cu_2S/TiO_2	Hydrothermal treatment	0.5M Na2SO4	-	-	24.1µmol/g	Applied Catalysis B: Environmental 254 (2019) 174–185182 [74]

Responsivity (R_λ): The responsivity of a photodetector is defined by following relation;

$$R_\lambda = \frac{J_{ph}}{A \times P_\lambda} \quad \textbf{(A/W)} \qquad \textbf{(1.7)}$$

Where, J_{ph}, P_λ, A is photocurrent density, the active area of the device, and power density.

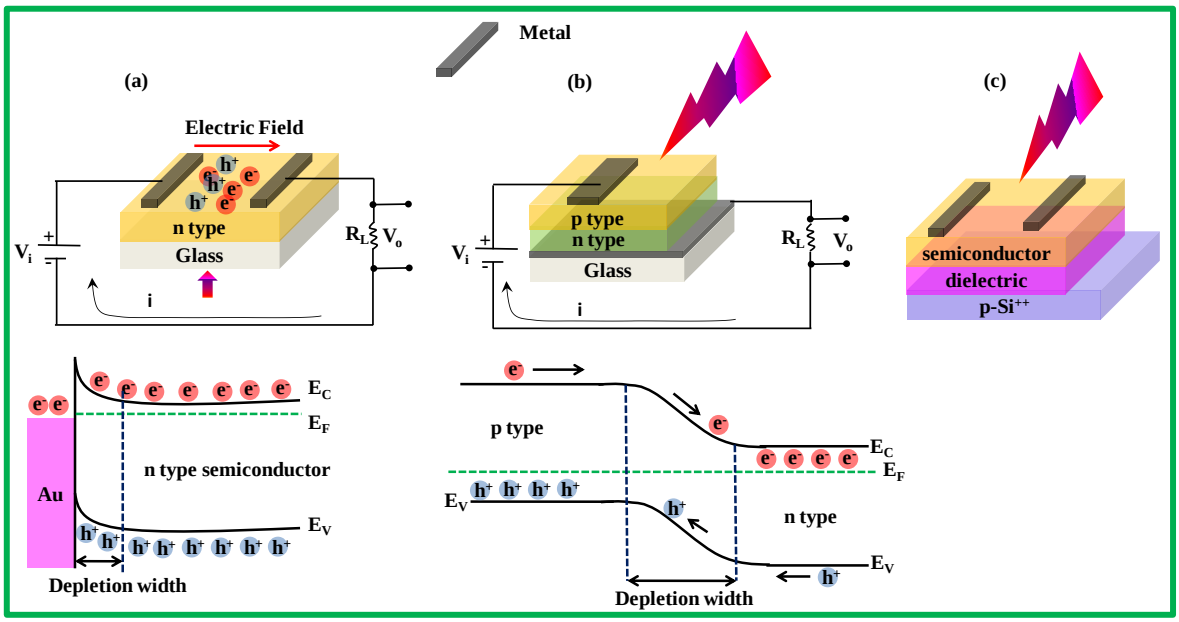

Figure 1.10: *The type of photodetector (a) Photoconductor, (b) Photodiode, and (c) Phototransistor*

External Quantum Efficiency (EQE): EQE is defined, the number of photogenerated charge carriers per unit incident photons [62], it is given by the equation (1.8)

$$\frac{Photogenerated\,number\,of\,charge\,carrier}{The\,number\,of\,incident\,photon} = \frac{J_{ph}}{e\emptyset} = \frac{J_{ph}\times h\nu}{eP_o} = \frac{hc\times R_\lambda}{e\lambda} \times 100 \qquad (1.8)$$

Where, h, ν, c, P_o, e, $\emptyset$ *and* λ is plank constant, frequency, speed of light, output power, electronic charge, the flux of incident photon and wavelength of the incident light.

Detectivity (D*): The detectivity of the device has defined the measure of the signal to noise ratio of the photodetector over the 1 Hz bandwidth normalized to the device area[62], shown in the equation (1.9)

$$\mathbf{D^*} = \frac{\sqrt{AB}}{NEP} = \frac{R_\lambda}{\sqrt{(2eJ_d)}} \qquad (1.9)$$

Where, B, NEP, and J_d are bandwidth, equivalent noise power.

1.7 Scope and objective of present work

The metal, metal oxide and metal sulfide NPs have varities of applications, including the photovoltaic device electrocatyst, photocatalysts (H_2 or O_2 evolutions), photoelectrocatalyst, biomedical application, sensor application etc. All these application of nanostructured material depends on their unique physical and chemical behavior those are originated due to their unusual small size. Again, behavior of nanoparticle can be tuned by doping with (cation/anion) and making heterojunctions with other materials. Particularly, in this thesis, we have modified different physical behavior of TiO_2 by forming metal/metal oxide and different band gap metal sulphide/metal oxide heterojunction formation and has been utilized for photoanode fabrication of photoelectrochemical H_2 generation and visible light photodetector fabrication. Therefore, the objectives of my PhD work are;

- Understanding and synthesis of plasmonic silver nanoparticle (Ag NPs) within TiO_2 thin film by solution processed *in situ* growth technique and its application as photoanode for photoelectrochemical H_2 evolution.
- Synthesis and fabrication of silver sulfides, (Ag_2S) NPs within TiO_2 thin film and photoanode fabrication for photoelectrochemical H_2 evolution. Growth of copper sulfide (Cu_2S) NPs within TiO_2 thin film and its application for photoanode and photodetector fabrication which have been used for photoelectrochemical H_2 evolution and visible light detection.

In chapter 2 will discuss the synthesis and characterization technique for the in-situ grown NPs inside TiO_2 thin film. Also, solution processed fabrication technique of $Li_4Ti_5O_{12}$, TiO_2, Ag-TiO_2, Ag_2S-TiO_2, Cu_2S-TiO_2 and Cu_2S-TiO_2/ZnO thin films.

Chapter 3 describes the direct evidence of an efficient plasmon-induced hot-electron transfer process at an *in situ* grown Ag/TiO_2 interface that has been utilized for highly enhanced solar H_2 generation**.** This Ag/TiO_2 heterojunction growth technique requires three successive steps that include the fabrication of $Li_4Ti_5O_{12}$ ceramic thin film by sol-gel technique followed by an ion-exchange process that replaces Li^+ by Ag^+ to form $Ag_4Ti_5O_{12}$ thin film. Finally, $Ag_4Ti_5O_{12}$ thin-film converted to Ag -TiO_2 nanocomposite due to the reduction process of Ag^+ to Ag^o. Such kind of *in situ* growth of Ag NP inside TiO_2 matrix allows larger interface area formation between Ag NPs and TiO_2 with lesser interface trap state. Formation of Ag-TiO_2 was confirmed by SEM, XRD, XPS and UV-VIS absorption study. Plasmon-induced hot electron generation and its efficient transfer to the conduction band (CB) of neighboring metal oxide is an effective route to photoelectrochemical solar energy harvesting application. Photoelectrochemical measurement of an optimized Ag(NPs)-TiO_2 thin film photoanodes showed a high photocurrent generation of density 42 mA cm^{-2} in 1M KOH solution under , which is three orders higher than pure TiO_2 and stable for more than 1.5 hours. These data indicates it's an excellent potential application for photoelectrochemical (PEC) water splitting with high stability. This current density is significantly higher than the recently reported Ag/TiO_2 system. Again, the IPCE spectrum in visible range shows a strong photocurrent generation in the region of plasmonic absorption of Ag NPs. This result reveals that the major contribution to solar hydrogen generation is coming from the Plasmon-induced hot-electrons.

In Chapter 4 we will describe the Role of electronically coupled *in situ* grown silver sulfides (Ag_2S) nanoparticles with TiO_2 for the efficient photoelectrochemical H_2 evolution. A solution-processed *in situ* grown synthesis method has been developed to

grow of silver sulfide (Ag_2S) nanoparticles (NPs) inside a titanium oxide (TiO_2) thin film and has been utilized for electro-photocatalytic H_2 generation. This thin film growth requires three successive steps, including sol-gel, derived ion-conducting thin film fabrication containing loosely bound light ion (Li^+) followed by ion-exchange (with $Li^+ \leftrightarrow Ag^+$) and subsequent sulfurization process. This entire solution-processed deposition technique is capable of fabricating cost-effective large area Ag_2S-TiO_2 heterojunction thin film containing Ag_2S NPs ranging ~ 10-70 nm. This Ag_2S-TiO_2 thin film is grown on three different substrates, including fluorine-doped tin oxide (FTO), FTO/TiO_2 (sol-gel), and FTO/TiO_2 (NP) coated glass. A comparative photo-electrocatalytic measurement of these Ag_2S (NPs)-TiO_2 thin film photoanodes showed that sample on FTO/TiO_2 (NP) coated glass generate highest photocurrent of density ~50 mA cm^{-2} at 0.5 V vs. NHE in 1M KOH solution which is three orders higher than pure TiO_2 and stable for more than 1.5 hours, indicating it's excellent potential application for photoelectrochemical (PEC) water splitting. The photocurrent generation of this Ag_2S-TiO_2 thin film is significantly higher than earlier reported Ag_2S-TiO_2 system, which originated due to the reduced carrier recombination from Ag_2S/TiO_2 interface trap state of such *in situ* grown Ag_2S NPs. Volumetric measurement shows that this generation rate is ~ 90±5 μmol/cm^2/hour. This current density is significantly higher than the earlier reported Ag_2S/TiO_2 system. Moreover, this photocurrent shows good stability that has been tested for more than 1.5 hours

Chapter 5 describes the *in situ* grown electronically coupled Cu_2S-TiO_2 heterojunction thin film for the efficient H_2 evolution via water splitting. We have developed a solution-processed technique for an *in-situ* grown Cu_2S-TiO_2 nanocomposite thin film that has been

utilized for efficient H_2 generation through water splitting. Like Ag_2S/TiO_2 heterojunction thin film, this Cu_2S-TiO_2 growth process also consists of three successive steps. In the beginning, sol-gel derived ion-conducting $Ag_4Ti_5O_{12}$ thin-film was fabricated followed by ion-exchanged with $Li^+ \leftrightarrow Cu^+$ and subsequent sulfurization process. Similar to earlier study, this Cu_2S-TiO_2 thin film was grown on three different substrates, including FTO, TiO_2 (Sol-gel)/FTO, and TiO_2 (NP)/FTO coated glass substrates and have been used as photoanode for water splitting. A comparative photo-electrocatalytic measurement shows that the highest photocurrent can be obtained by Cu_2S-TiO_2/TiO_2 NPs/FTO photoanode with a current density of~36 mA cm^{-2} at 0.5 V potential (E Vs REH) in 1M KOH solution. Moreover, this photocurrent is stable for more than 3 hours, indicates its excellent potential application for photoelectrochemical (PEC) water splitting. This photocurrent generation of these photoanode thin films is significantly higher than earlier reported Cu_2S (NPs.)-TiO_2 nanocomposite photoanodes, which is originated due to the reduced carrier recombination by *in-situ* grown, electronically coupled Cu_2S-TiO_2 heterojunction interface. Volumetric measurement shows that this H_2 generation rate is ~55±5 μmol/cm^2/hour.

Chapter 6 describe the visible light photodetector fabrication by using *in situ* growth of Cu_2S/TiO_2 heterojunction. This Cu_2S/TiO_2 heterojunction thin film has been fabricated on top of a glass substrate exactly in same way as mention in chapter 5. For better sensitivity device has been fabricated with ZnO underlying layer with a device architecture Al/Cu_2S-TiO_2/ZnO/glass. This lateral heterojunction photodetector shows a detectivity of 2.23×10^{11} jones. The transient time response of this device raising and falling time are 7.11 and 8.21 seconds respectively, which is reasonably good for the photoconductor device.

Chapter 7 will discuss the conclusion of PhD thesis and future scope of this thesis work